

UNCLASSIFIED

AD 4 6 4 7 0 1

DEFENSE DOCUMENTATION CENTER

FOR

SCIENTIFIC AND TECHNICAL INFORMATION

CAMERON STATION ALEXANDRIA, VIRGINIA



UNCLASSIFIED

NOTICE: When government or other drawings, specifications or other data are used for any purpose other than in connection with a definitely related government procurement operation, the U. S. Government thereby incurs no responsibility, nor any obligation whatsoever; and the fact that the Government may have formulated, furnished, or in any way supplied the said drawings, specifications, or other data is not to be regarded by implication or otherwise as in any manner licensing the holder or any other person or corporation, or conveying any rights or permission to manufacture, use or sell any patented invention that may in any way be related thereto.

AD NO. 464701

464701

RECEIVED COPY

(To be submitted to Physics Letters)

⑭ Rept. no. HEPL - 365

⑪ Feb 1965

② FINE STRUCTURE OF THE GIANT DIPOLE RESONANCE IN O^{16} AS OBSERVED BY
INELASTIC ELECTRON SCATTERING AT 180° DEGREES.

⑩ by Georges Vanpraet.
⑤ High Energy Physics Lab
Stanford University, Calif.
~~Stanford, California~~

DDC
JUN 15 1965

⑮ Contract Nonr. 22567-1

- * Work supported in part by the Office of Naval Research
- † On leave from the Interuniversity Institute for Nuclear Sciences, Natuurkundig Laboratorium, University of Gent, Belgium.

mk

(To be submitted to Physics Letters)

HEPL - 365

February 1965

FINE STRUCTURE OF THE GIANT DIPOLE RESONANCE IN O^{16} AS OBSERVED BY
INELASTIC ELECTRON SCATTERING AT 180° *

Georges Vanpraet [†]

High Energy Physics Laboratory

Stanford University

Stanford, California

New experimental work has been devoted to the excitation of the nuclear giant dipole resonance in O^{16} by scattering of electrons with incident energies of 43, 59 and 69 MeV. Higher resolution measurements revealed more structure in the energy distribution of electrons inelastically scattered through 180° . The advantages of using inelastic electron scattering to excite the giant resonance have been discussed previously^{1,2}. Lewis and Walecka³ showed that form factors measured in this way provide a much more sensitive test of any theory of the giant resonance than other techniques.

In first Born approximation ($Z/137 \ll 1$), neglecting both nuclear recoil and the electron mass in comparison with the electron energy, the differential cross section at 180° for excitation of the giant dipole resonance is reduced to the expression^{4,3}:

$$\frac{d\sigma}{d\Omega} = \frac{\pi\alpha^2}{K_1^2} \left| \langle J = 1^- || T_1^{el}(q) || J = 0^+ \rangle \right|^2$$

where:

α = fine structure constant,

K_1 = the initial electron wave number,

$\hbar q$ = the three-momentum transferred to the nucleus, and

$T_1^{el}(q)$ = the transverse electric dipole operator containing
the nuclear current and magnetization density operators.

Lewis⁵ calculated the reduced transition matrix element or inelastic transverse form factor for electromagnetic excitation of the giant resonance in O^{16} on the basis of several different models. He has found that the squared form factor for the combined strength of the main giant resonance, around 24 MeV in this nucleus, has a characteristic shape when plotted as a function of momentum transfer. The results agreed with the experimental data of Goldemberg and Barber². The prediction of the theory concerning a shift of the main dipole strength from the lower to the higher energy states of the giant resonance with increasing q values, seemed also to be confirmed experimentally.

△ The purpose of this paper is to report results of higher resolution measurements on O^{16} using the Stanford Mark II linear accelerator. △ Although we now observe more states than predicted by the theory, the sum of the cross section in the giant resonance region plotted as a function of momentum transfer q , behaves as predicted by the particle-hole calculations. However, the change in the structure of the giant resonance cross section as the momentum transfer is varied is not so simple as in the lower resolution experiments².

The experimental equipment was described previously^{6,2}. For the present measurements, some improvements to the accelerator and pulse forming network made the operation of the equipment more reliable than before. For O^{16} , a distilled water target of 0.160 g/cm^2 (0.005 radiation length) was used. The water was contained between two 3μ stainless steel foils. Fig. 1 shows a typical spectrum of 69 MeV electrons scattered at 180° . Other spectra have been taken at 59 and 43 MeV primary energies. The absolute cross sections, determined by comparison with the proton elastic cross section, are plotted in Fig. 2 as a function of the excitation energy,

after being corrected for the radiative effects associated with electron scattering^{7,8,2}. It is clear that the number of states observed, even below the giant resonance region is much higher than was obtained before in 180° electron scattering. The existence of this fine structure in O^{16} has also been confirmed by the results of Isabelle and Bishop⁹ and the high resolution $O^{16}(\gamma, p)$, $O^{16}(\gamma, n)$ and $N^{15}(p, \gamma)$ experiments discussed in references¹⁰. The photon absorption results of Burgov et al¹¹ are also very valuable.

In the region between 19 and 27 MeV, the cross sections now display peaks at 19.2, 20.4, 21.5, 22, 22.8, 23.6, 24.5, 25.5 and 26 MeV. Some of them appear in each of the three measurements; the other are somewhat masked by the adjacent structure or they slightly shifted their position. The resonance energies of the peaks are regarded as energy levels excited in the giant resonance region of O^{16} . Their values are summarized in Table I and can be compared with levels observed by other techniques. However, we want to emphasize the peculiar fact that the exact excitation energies of some states given by the many investigators, differ from each other by an amount up to 0.5 MeV. From the experimental point of view, a possible reason therefore is that the considerable structure in the spectra is sometimes quite difficult to identify in an unambiguous way with a certain excitation because the states involved can have large overlapping widths which are not in general well known. An attempt has been made to evaluate the form factor for each resolved level by fitting the peaks with resonance lines. The numerical results for the integrated cross section and the relevant matrix elements are also given in Table I.

In Figure 3 we show the square of the form factor for the main part of the giant resonance plotted as a function of q . The curves are calculated on the basis of the collective and the shell model, as explained in Lewis' paper^{5,13}. The experimental point at 23 MeV was obtained from results with photons. The other two solid circles at $q = 84 \frac{\text{MeV}}{c}$ and $116 \frac{\text{MeV}}{c}$ represent values from Goldemberg and Barber². The present experimental values of the matrix elements are represented by the triangles at momentum transfers 62, 94 and $114 \frac{\text{MeV}}{c}$, assuming also a mean excitation energy of 24 MeV for the kinematical calculations. They were obtained by integrating the cross sections from 19.5 to 27 MeV in order to cover the region made up of the three predicted giant resonance dipole states. The

two other ($J = 1^-$, $T = 1$) states and the properties of the levels observed below the giant resonance will be discussed elsewhere.

There is no doubt that the Goldhaber-Teller collective model fails to give the right magnitude and shape for the form factor. However, when we compare the three spectra of Fig. 2 with each other, it turns out, as q increases from 62 to 114 MeV/c, that the transfer in dipole strength between a state that carries most of the dipole strength and its next higher neighbor is not so pronounced as predicted by the theory (see Ref. 5, Fig. 2). Actually, for O^{16} the greater number of states in that region could obscure the effect of the dipole strength shift at higher q values. This is not possible in the case of C^{12} where only two dominating states are involved for the giant resonance. Since the photon data of Burgov et al.¹¹ do not show any dominating level excitation below 21 MeV, we might as well integrate the electron cross sections from 21 up to 27 MeV. If we divide the giant resonance region into a lower and higher energy part at an arbitrary energy of 23.5 MeV, we can compare the spectra as far as the distribution of the dipole strength is concerned. We find that for the photon absorption spectrum¹¹, the ratio of the strength of the high energy region to that of the lower energy part is ~ 0.64 . This ratio becomes for the electron data respectively 0.82, 1.4 and 1.35 for increasing q -values. These ratios agree fairly well with Lewis's prediction for the shift of the dipole strength. However, for the highest value of the momentum transfer, the ratio did not increase as predicted. This can be explained by the fact that in the lower energy region, probably not all of the transition strength observed, arises from E_1 transitions. At these values of q , higher multipole order contributions can become important¹².

We conclude that the particle-hole description of the giant resonance of O^{16} is consistent in predicting the over-all strength of the dipole states. However, further theoretical work and perhaps measurements extended over a higher range of momentum transfers and μ -capture experiments¹⁴ on O^{16} could be helpful for explaining the additional structure to the dominant dipole states of the giant resonance in O^{16} .

I wish to thank Professor W. C. Barber for his constant encouragement and advice, and for his hospitality in making the facilities of the High Energy Physics Laboratory available to me. I wish also to acknowledge

Professor J. D. Walecka and Mr. T. deForest for stimulating discussions. Finally, I am indebted to Dr. P. Kossanyi for helping in analyzing the data.

FOOTNOTES

- * Work supported in part by the Office of Naval Research [Nonr 225(67)].
- † On leave from the Interuniversity Institute for Nuclear Sciences, Natuurkundig Laboratorium, University of Gent, Belgium.

REFERENCES

1. W. C. Barber, Ann. Rev. Nuclear Sci. 12, 1 (1962).
2. J. Goldemberg and W. C. Barber, Phys. Rev. 134, B963 (1964).
3. F. H. Lewis, Jr. and J. D. Walecka, Phys. Rev. 133, B849, (1964).
4. F. H. Lewis, Jr., J. D. Walecka, J. Goldemberg and W. C. Barber, Phys. Rev. Letters 10, 493 (1963).
5. F. Lewis, Jr., Phys. Rev. 134, B331 (1964).
6. W. C. Barber, J. Goldemberg, G. A. Peterson and V. Torisuka, Nucl Phys. 41, 461 (1963).
7. Y. S. Tsai, Phys. Rev. 122, 1898 (1961).
8. F. Ginzberg and R. H. Pratt, Phys. Rev. 134, B773 (1964).
9. D. B. Isabelle and G. R. Bishop, Nucl. Phys. 45, 209 (1963).
10. E. Finckh, R. Kosiek, K. Lindenberger, K. Maier, U. Meyer-Berkhout, M. Schechter and J. Zimmerer, Z. Physik 174, 337 (1963).
N. W. Tanner, G. C. Thomas and E. D. Earle, Nucl. Phys. 52, 45 (1964).
11. N. Burgov, G. Darrilyan, B. Dolbinkin, L. Lasaceva and F. Nikolaev, Soviet Phys. JETP 16, 50 (1963).
12. J. D. Walecka and T. deForest (private communication).
13. F. Lewis, Jr., Erratum (to be published and private communication).
14. J. Barlow, J. Sens, P. Duke and M. Kemp, Phys. Lett. 9, 84 (1964).

FIGURE CAPTIONS

- Figure 1. Energy distribution of 69 MeV electrons scattered inelastically through 180° from a water target.
- Figure 2. Cross section for inelastic scattering of electrons at 180° with excitation of the O^{16} nucleus, plotted as a function of excitation energy.
- Figure 3. Square of the form factor for the O^{16} giant dipole resonance, plotted as a function of momentum transfer. The experimental point at 23 MeV is from photon work. The new experimental values from 180° electron scattering are represented by the triangles. The curves are calculated on the basis of different nuclear models (ref. 5, 13).

TABLE I
Cross sections and matrix elements of levels observed
in the ^{16}O giant resonance region.

EXPERIMENTAL LEVELS (± 0.25 MeV)	$\frac{d\sigma}{d\Omega} \times 10^{32}$ (cm ² /sr)	$ \langle J_f T(q) J_i \rangle ^2 \times 10^3$
43 MeV	19.2	1.8 \pm 0.27
	20.4	1.85 \pm 0.28
	21.5	4.5 \pm 0.7
	22.8	2.6 \pm 0.4
	23.9	5.8 \pm 0.9
	24.5	
59 MeV	19.2	1.5 \pm 0.18
	20.4	1.85 \pm 0.22
	22.0	2.12 \pm 0.25
	22.8	1.0 \pm 0.12
	23.6	1.8 \pm 0.22
	25.5	1.9 \pm 0.23
	26.7	0.7 \pm 0.09
69 MeV	19	1.6 \pm 0.16
	20.2	2.15 \pm 0.22
	22	2.27 \pm 0.23
	23	0.68 \pm 0.07
	23.6	1.41 \pm 0.14
	24.5	1.18 \pm 0.12
	26	1.4 \pm 0.14

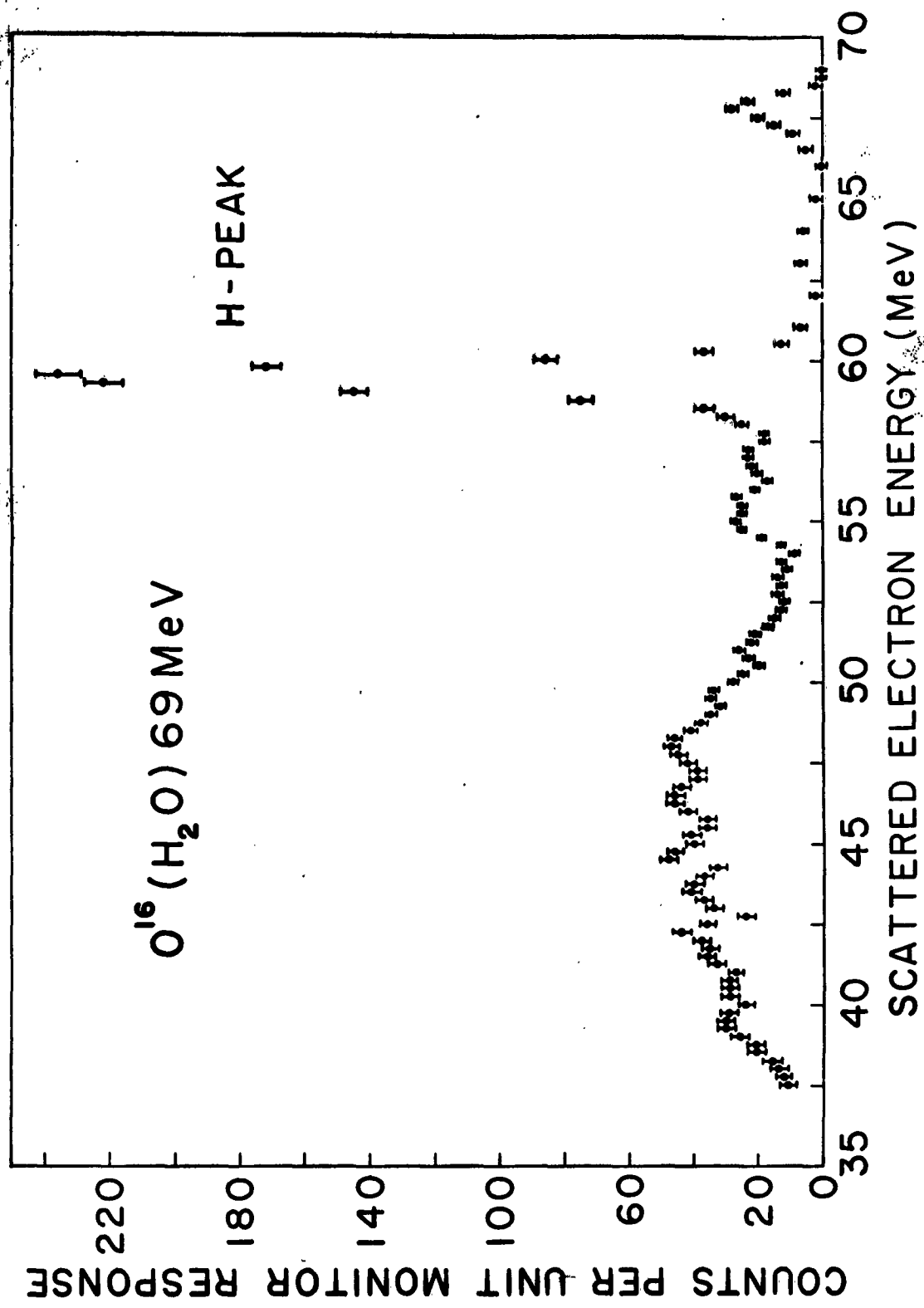


FIGURE 1

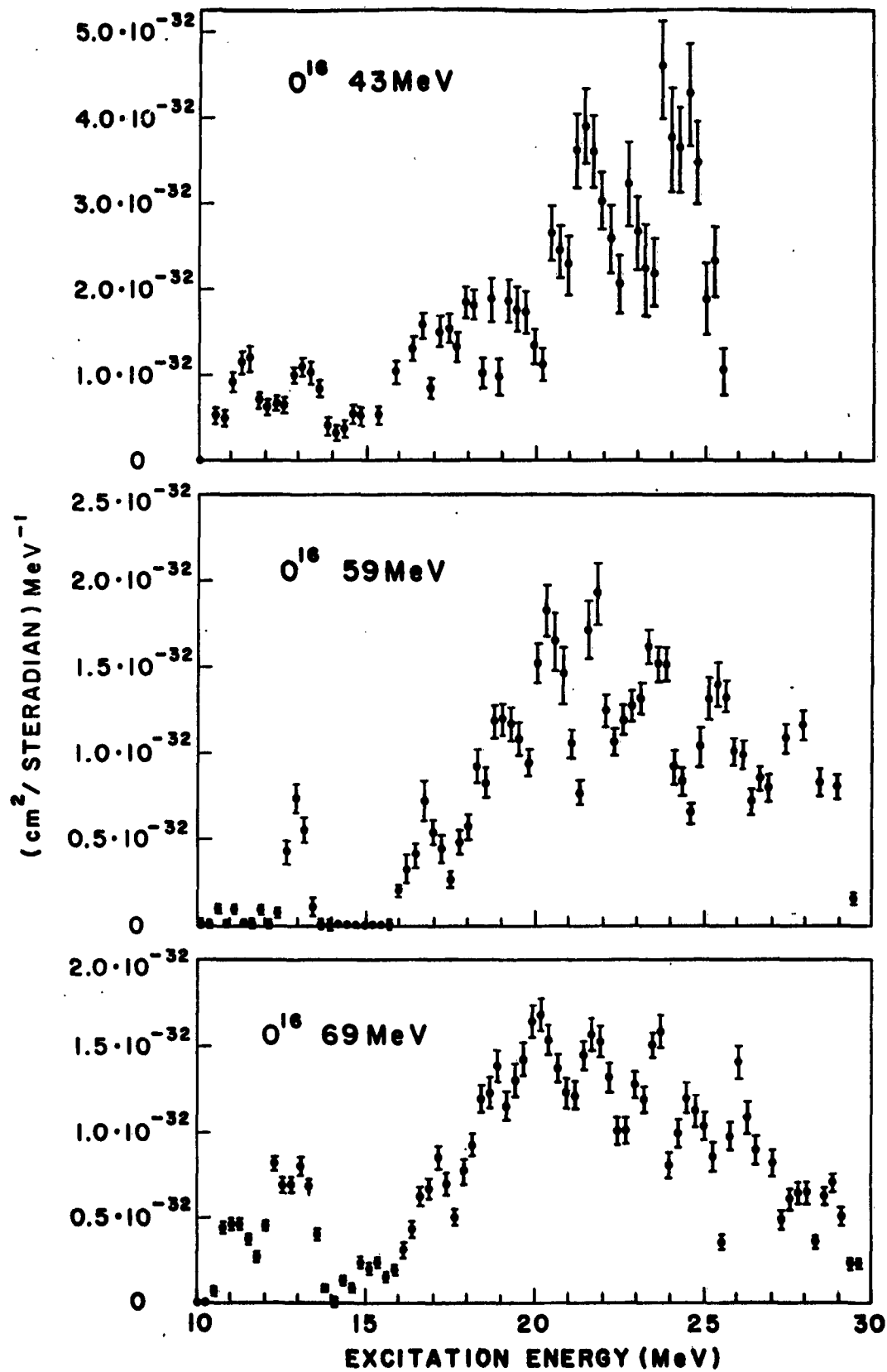


FIGURE 2

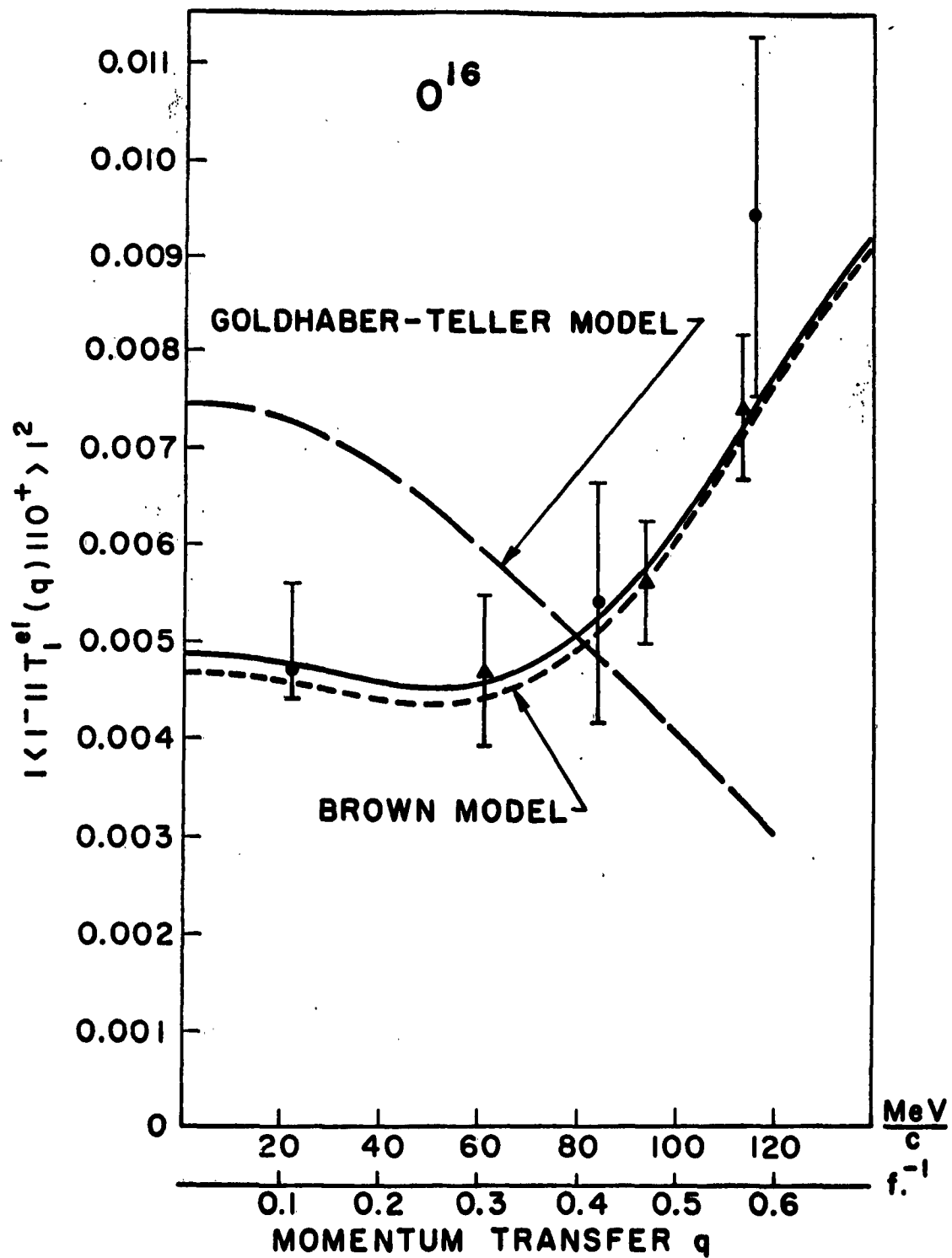


FIGURE 3